

Li nonstoichiometry and crystal growth of an untwinned one-dimensional quantum spin system $\text{Li}_x\text{Cu}_2\text{O}_2$

H. C. Hsu,^{1,2} H. L. Liu,² and F. C. Chou^{1,3,*}¹Center for Condensed Matter Sciences, National Taiwan University, Taipei 10617, Taiwan²Department of Physics, National Taiwan Normal University, Taipei 116, Taiwan³National Synchrotron Radiation Research Center, HsinChu 30076, Taiwan

(Received 27 August 2008; revised manuscript received 3 November 2008; published 1 December 2008)

Floating-zone growth of untwinned single crystal of $\text{Li}_x\text{Cu}_2\text{O}_2$ with high Li content of $x \sim 0.99 \pm 0.03$ is reported. Li content of $\text{Li}_x\text{Cu}_2\text{O}_2$ has been determined accurately through combined iodometric titration and thermogravimetric (TGA) methods, which also ruled out the speculation of chemical disorder between Li and Cu ions. The morphology and physical properties of single crystals obtained from slowing-cooling and floating-zone methods are compared. The floating-zone growth under $\text{Ar}/\text{O}_2=7:1$ gas mixture at 0.64 MPa produces large area of untwinned crystal with highest Li content, which has the lowest helimagnetic ordering temperature ~ 19 K in the $\text{Li}_x\text{Cu}_2\text{O}_2$ system.

DOI: [10.1103/PhysRevB.78.212401](https://doi.org/10.1103/PhysRevB.78.212401)

PACS number(s): 75.10.Pq, 75.30.Hx, 74.25.Ha

$\text{Li}_x\text{Cu}_2\text{O}_2$ has a Cu-O chain structure formed with edge-sharing CuO_4 plaquettes in the ab plane while these chains are connected through CuO_2 dumbbells along the c direction.¹ This compound is uniquely composed of nearly equal amount of Cu^{1+} and Cu^{2+} simply from the consideration of charge balance, where O-Cu-O dumbbells are formed with Cu^{1+} . The crystal structure was initially misidentified as a tetragonal symmetry due its severe twinning until it is refined with an orthorhombic symmetry of $a \sim 2b$.^{1,2} Helimagnetic ordering has been identified by neutron scattering along the b direction with an incommensurate propagation vector $(0.5, \xi=0.174, 0)$, where the spin spiral plane is proposed to lie in the ab plane with pitching angle of $2\pi\xi \sim 62.6^\circ$,³ although the existence of transverse spin component in the bc plane is confirmed by Seki *et al.* later.⁴ Competing quantum and classical spin periodicity has been explored by neutron scattering, but the proposed important role of intrinsic chemical disorder in this one-dimensional (1D) quantum spin system has not been examined fully yet.³

The importance of $\text{Li}_x\text{Cu}_2\text{O}_2$ compound has regenerated great interest in the condensed-matter physics community after it is identified as the first cuprate system with multiferroic behavior by Park *et al.*⁵ Spontaneous electric polarization emerges below the helimagnetic ordering temperature around ~ 22 K and the direction of polarization can be changed by the applied field. However, due to the low atomic number of Li which prevents precise Li content determination, theoretical models that are applied to interpret the origin of multiferroic behavior are based mostly on the as-grown slow-cooled plus high-temperature quenched single-crystal LiCu_2O_2 .⁶ The nominal stoichiometry lacks precise Li and Cu contents analysis, which makes the interpretation of these phenomena complicated, especially when the level of Cu^{2+} impurity spin is the key parameter on interchain interaction.^{3,7} In particular, the slow-cooling growth method that accompanies high-temperature quenching in the air produces crystals with severe twinning and potential chemical disordering due to the similar ionic size between Li^+ and Cu^+ . The correlation between ferroelectricity and magnetic ordering and the competition between classical and quantum

spins are clearly the most important questions in current 1D spin $\frac{1}{2}$ system. In order to clarify issues from materials point of view, which is vital on constructing an accurate theoretical model, we present details of crystal growth, Li/Cu content analysis and helimagnetic ordering transition analysis based on magnetic-susceptibility measurement in this Brief Report.

Due to the low atomic number limitation, Li content cannot be determined accurately using either inductive coupled plasma (ICP) or electron probe microanalysis (EPMA) techniques. Li content, which is closely connected to the $\text{Cu}^+/\text{Cu}^{2+}$ ratio, has never been addressed carefully with confidence before. Exact Li and Cu contents have been extracted convincingly by combined iodometric titration and thermogravimetric analysis in this study. Contrary to the previous estimate of copper deficiency and the speculated chemical disorder between Li and Cu,⁶ we find that the Cu content is close to 2 and Li content is found to be lower than 1 always, which strongly suggests that the doped Cu^{2+} quantum spins that bridge the CuO_2 ribbons between layers are originated from Li deficiency. Herein we report on detailed chemical analysis, Li level modification, and characterization on nominal LiCu_2O_2 crystals grown from slow-cooling and floating-zone methods. Direct correlation between Li nonstoichiometry and the helimagnetic ordering transition temperature is implied from our current study.

Floating-zone crystal (called FZ) has been grown from the feed rod prepared with $\text{Li}_2\text{CO}_3/\text{CuO}$ mixture of molar ratio 1.2:4 and the cold-pressed feed rod of $10 \text{ cm} \times \varnothing 6 \text{ mm}$ is annealed at 850°C for 12 h under the oxygen flow. The 20% excess of Li content is used to compensate for the high-temperature Li vapor loss and the crystal growth is presumably through the congruent melt of the feed rod directly. The optimum growth rate has been found to be 3 mm/hr and a 20 rpm rotation is maintained. Various gas environments of different Ar/O₂ ratios have been tested in order to achieve single phase growth with specific Li content. Slow-cooled crystal (called SL) following recipe reported by Bush *et al.*⁶ is prepared. Final Li content can also be tuned through vacuum annealing starting from the as-grown FZ or SL crystals. The crystals are sealed within an evacuated quartz tube

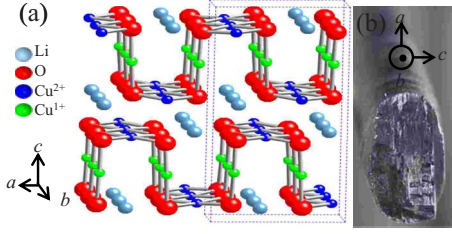
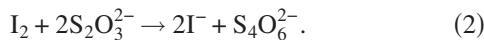
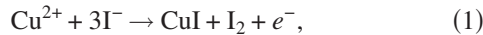


FIG. 1. (Color online) (a) Crystal structure of LiCu_2O_2 , where the magnetic Cu^{2+} ion is shown in blue and the nonmagnetic Cu^{1+} is in green. (b) A typical FZ crystal grown under $\text{Ar}/\text{O}_2=7:1$ gas mixture of 0.64 MPa. Note that the crystal grows into an elliptical cross section with flat ab plane after the first centimeter pulling and the growth direction is along the b axis.

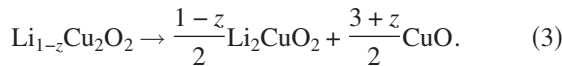
and annealed at 400 °C and 600 °C for 6–24 h, respectively [called SL-(4)600 and FZ-(4)600]. There is white deposit generated inside the quartz tubing after the vacuum annealing, presumably due to the Li vapor loss which is strongly temperature dependent.

Iodometric titration is performed to estimate the $\text{Cu}^+/\text{Cu}^{2+}$ ratio. Since only Cu^{2+} has the oxidation power and the sample contains nearly half of $\text{Cu}^+/\text{f.u.}$, a two-step titration procedure is applied. In the first step, single-crystal sample is ground and dissolved in 1 M HCl boiled for 5 min to ensure that all Cu^+ is converted into Cu^{2+} , and excess KI is added to the solution before titration proceeds under N_2 flow, while in the second step titration is performed without the boiling procedure so that only the Cu^{2+} portion is determined. The amount of Cu^{2+} in the solution can be determined indirectly through the iodine content titrated with 0.1 M $\text{Na}_2\text{S}_2\text{O}_3$ using deflecting point of the electric potential as the indicator of titration ending point. The complete reaction steps include



The Li content can be estimated from $\text{Li}_{1-z}\text{Cu}_{1-z}\text{Cu}_{1+z}^{2+}\text{O}_2$ formula after the total copper content is normalized to $2/\text{f.u.}$

Thermogravimetric decomposition method is applied to determine the Li content and compare with that from titration. $\text{Li}_{1-z}\text{Cu}_2\text{O}_2$ can be decomposed into Li_2CuO_2 and CuO under oxygen flow as



Li content can be calculated from the weight gain after the sample is converted into Li_2CuO_2 and CuO completely. Since titration method requires much more sample in powder form to increase the accuracy, TGA decomposition method has been used to determine the Li content of single crystal effectively in this Brief Report, although it has a larger error bar of ± 0.03 and is systematically higher than that from titration by about 0.02.

Magnetic susceptibility is measured with superconducting quantum interference device (SQUID) magnetometer (Quantum Design MPMS-XL) with a field of 1 kOe for magnetic

TABLE I. Growth conditions and products for floating-zone growth of $\text{Li}_x\text{Cu}_2\text{O}_2$.

Sample	Li content (TGA)	Ar:O ₂	Compound(s)
SL	0.87 ± 0.03	Air	$\text{Li}_x\text{Cu}_2\text{O}_2$
FZ-1		5:1	$\text{Li}_x\text{Cu}_2\text{O}_2 + \sim 2\%\text{LiCu}_3\text{O}_3$
FZ-2	0.99 ± 0.03	7:1	$\text{Li}_x\text{Cu}_2\text{O}_2$
FZ-3	0.95 ± 0.03	10:1	$\text{Li}_x\text{Cu}_2\text{O}_2$
FZ-4	0.84 ± 0.03	Ar	$\text{Li}_x\text{Cu}_2\text{O}_2$

field applied along and perpendicular to the ab plane. Since the spin susceptibility of helimagnetic ordering varies smoothly comparing with the conventional ferromagnetic (FM) or antiferromagnetic (AFM) ordering, $d\chi/dT$ instead of χ versus temperature is used to identify the magnetic phase transition.

We have tested the floating-zone growth under various growth conditions in order to control the Li content and summarized in Table I. The higher gas pressure of 0.64 MPa reduces Li vapor loss significantly, although the Li content and impurity level are also closely related to the oxygen partial pressure. Single phase crystal of highest Li content is obtained under $\text{Ar}/\text{O}_2=7:1$ gas environment.

Figure 1(b) shows the typical FZ crystal grown under $\text{Ar}/\text{O}_2=7:1$ gas mixture of 0.64 MPa. The FZ crystal shows flat surface after the first ~ 1 cm pulling and the flat surface is verified by x-ray diffraction to be the ab plane, i.e., the plane that contains CuO_4 plaquettes as shown in Fig. 1(a). Crystal surface images taken by polarized light are displayed in Fig. 2 for both FZ and SL crystals. Note that the area of the dark-light contrast of Figs. 2(a) and 2(b) for FZ crystal and Figs. 2(c) and 2(d) for SL crystal has different scales, where FZ crystal shows large untwinned area of $\sim 3 \times 3$ mm², which is more than 100 times larger than the severely twinned SL crystal. There is only stripelike second domain observed sporadically on the FZ crystal surface as shown in Fig. 1(b). The FZ crystal-growth direction follows closely to the edge-shared CuO_4 plaquettes, i.e., the spiral spin chain b -axis direction.³ Mirror plane of (210) which is parallel to the domain boundary is clearly indicated by the highlighted lines in Figs. 2(a) and 2(b), in agreement with the proposed $a \sim 2b$ structure model.

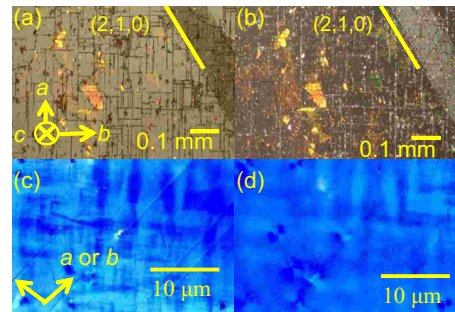


FIG. 2. (Color online) (a) and (b) are optical microscope images of FZ crystal taken with depolarized light of 90° difference. Similarly (c) and (d) are taken from SL crystal.

TABLE II. Comparison of Cu content obtained from iodometric titration and predicted calculation.

Sample	Cu by titration (mol)	Cu from calculation (mol)
SL (15 mg)	$(1.81 \pm 0.03) \times 10^{-4}$	$(1.8068 \pm 0.014) \times 10^{-4}$
FZ (10 mg)	$(1.235 \pm 0.02) \times 10^{-4}$	$(1.2045 \pm 0.012) \times 10^{-4}$

The $\text{Cu}^+/\text{Cu}^{2+}$ ratio can be determined by combined iodometric titration and TGA decomposition techniques accurately. However, the Cu and oxygen contents should be addressed first while we must use an accurate formula unit in the calculation, in particular, before the possibility that Li^+/Cu^+ chemical disorder is not ruled out yet.⁶ We tentatively assign the formula unit of the sample to be LiCu_2O_2 , calculate the predicted total copper content, and compare with that obtained from titration. The titrated total copper content is obtained after a boiling procedure, as described in the experimental section, in order to convert all copper ions into Cu^{2+} state. The copper content based on LiCu_2O_2 formula weight and its predicted titration level is compared with the experimental results as shown in Table II. We find that the Cu content which is converted from the titrated $\text{Na}_2\text{S}_2\text{O}_3$ volume is nearly the same as the calculated values from predicted level using LiCu_2O_2 formula, which implies that the assumed copper content of 2 is correct. In addition, the assumption of Cu to be 2/f.u. holds true for crystals grown from both FZ and SL methods, which is against the possibility of Li^+/Cu^+ chemical disorder while two different degrees of quenching have been applied. The consistency displayed in Table II also supports the assumption about oxygen content to be close to 2 within 2% error. ICP analysis on NaCu_2O_2 shows Cu content to be 2 ± 0.02 also while it has a similar structure with a slightly lower magnetic transition temperature only.⁸ In addition, oxygen nonstoichiometry can be reasonably ruled out due to its significant stability between 890 °C and 1050 °C as reported by Bush *et al.*⁶

Titration results that determine the $\text{Cu}^+/\text{Cu}^{2+}$ ratio for two samples prepared by FZ and SL methods are summarized in Table III. We can easily convert the titrated $\text{Cu}^+/\text{Cu}^{2+}$ ratio to Li content through charge neutrality requirement with the predicted $\text{Li}_{1-z}\text{Cu}_{1-z}^+\text{Cu}_{1+z}^{2+}\text{O}_2$ formula, where total copper content is normalized to 2. Li content is obtained to be 0.838 ± 0.01 and 0.964 ± 0.015 for SL and FZ samples, respectively. We find that the Li content of SL growth is highly reproducible. The Li content near 0.83 could have a special

TABLE III. Li content of $\text{Li}_{1-z}\text{Cu}_{1-z}^+\text{Cu}_{1+z}^{2+}\text{O}_2$ derived from titrated $\text{Cu}^{2+}/\text{Cu}^+$ ratio with total Cu normalized to 2.

Titration No.	$1-z$ (FZ)	$\text{Cu}^{2+}/\text{Cu}^+$ (FZ)	$1-z$ (SL)	$\text{Cu}^{2+}/\text{Cu}^+$ (SL)
1	0.96	52/48%	0.83	58.5/41.5%
2	0.96	52/48%	0.83	58.5/41.5%
3	0.96	52/48%	0.84	58/42%
4	0.96	52/48%	0.84	58/42%
5	0.95	52.5/47.5%	0.84	58/42%

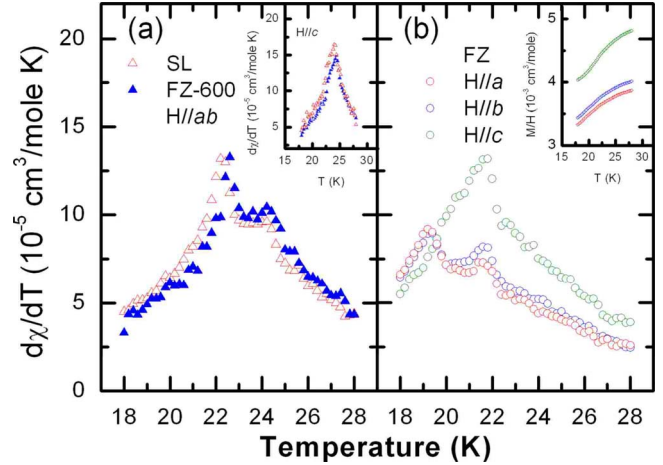


FIG. 3. (Color online) (a) Temperature-dependent $d\chi/dT$ of $\text{Li}_x\text{Cu}_2\text{O}_2$ for samples prepared from SL and 600 °C vacuum-annealed FZ sample (FZ-600). $H||c$ data are shown in the inset. (b) $d\chi/dT$ for the as-grown crystal FZ with highest $x \sim 0.99$. The original data $\chi(T)$ are shown in the inset.

stability. In particular its magnetic transition represented by the $d\chi/dT$ peak shape [see Fig. 3(a) below] is sharp and reproducibly similar to those reported in the literature.⁴ $\text{Li}_x\text{Cu}_2\text{O}_2$ is able to decompose into Li_2CuO_2 and CuO under oxygen environment and the Li content can also be calculated following Eq. (3) described above. Li content determined by TGA shows larger error bar and is consistently higher than that obtained from titration by ~ 0.02 . Although titration provides values of higher consistency and accuracy, significantly larger amount of sample in polycrystalline form is required. The Li content values reported in this Brief Report are based mainly on TGA results because of the limited sample size of annealed single-crystal samples.

Since the spin susceptibility of helimagnetic ordering varies smoothly comparing with that of the conventional FM or AFM ordering, $d\chi/dT$ instead of χ versus temperature for FZ samples is summarized in Fig. 3. We note the sample of FZ-600, which is prepared from the as-grown FZ crystal of $x \sim 0.99$ after 600 °C vacuum annealing, has identical Li content of ~ 0.84 and magnetic profile to that of the as-grown SL sample shown in Fig. 3(a), which suggests that physical properties must be critically determined by the Li content. Similar to what Seki *et al.*⁴ found, there are two anomalies near ~ 22.5 and 24 K for both ab and c directions, although 22.5 K is dominant for $H||ab$ and 24 K is dominant for $H||c$. Very importantly, spontaneous electric polarization is found only below 22.5 K.⁴ Since we can measure the spin susceptibility along a and b axes independently because of the sizable untwinned crystal, susceptibility data along three crystal axes for the as-grown FZ crystal ($x \sim 0.99$) are shown in Fig. 3(b). Similar two-peak profile near 19.2 and 21.7 K is found, which is about 2 K lower than those found in the SL sample and in the literature of identical growth method.³⁻⁵ The FZ sample of the highest Li content shows the lowest transition temperature, which is the lowest magnetic transition temperature found in this system so far. We find that there is no significant difference between a and b directions and the transition near 19.2 K is less pronounced as indicated

by the lower $d\chi/dT$ value. According to the similar $d\chi/dT$ profiles between a and b axes for the FZ crystal of the highest Li content, it would be reasonable to consider that spin spirals are in the ab plane in a classical picture, but further evidence is required to make a definite conclusion. It would be important to compare whether helimagnetic spiral modulation vectors are also different for the FZ and SL crystals. In addition, the existence of spontaneous electric polarization in the Li fully filled crystal must also be examined.

The Li-deficiency-induced Cu^{2+} impurity spins could be strongly correlated with the helimagnetic ordered spins within CuO_2 chains. Such strong impact of impurity spins to the host-ordered low-dimensional system has been observed in quasi-1D AF CaCu_2O_3 also.⁹ In particular, similar incommensurate ordering of Dy moments with the same periodicity as the Mn spiral ordering has been observed in the multiferroic DyMnO_3 .¹⁰ We speculate that the highly reproducible phase of particular stability from slow-cooling growth has a stoichiometry close to $\text{Li}_{0.83}\text{Cu}_2\text{O}_2$ always, and the $\sim 17\%$ Li^+ deficiency level implies that the introduced Cu^{2+} impurity could be directly correlated with the incommensurate ($\xi=0.174$) spiral modulation along the chain b direction.^{3,4} While each missing Li^+ ion would convert one Cu^+ to Cu^{2+} from the O-Cu-O dumbbell that bridges adjacent CuO_2 edge-sharing chains, the impurity Cu^{2+} would support

the nonrelativistic picture of multiferroicity model naturally as proposed by Moskvin *et al.*⁷ without even the need of founding their theory on the assumption of Cu deficiency and Li excess. On the other hand, the assumption of direct correlation among Li deficiency, Cu^{2+} impurity, helimagnetic ordering, and spontaneous electric polarization would require further rigorous cross checking. A complete study of spiral modulation vector and electric polarization based on the whole series of $\text{Li}_x\text{Cu}_2\text{O}_2$ is underway.

In conclusion, we have presented floating-zone growth of large untwinned $\text{Li}_x\text{Cu}_2\text{O}_2$ single crystal with controlled Li deficiency level from $0.75 \leq x \leq 0.99$. While Li and Cu contents are crucial in this compound and most chemical analyses failed to decide Li content, current combined titration and TGA studies provide a reliable way to determine the Li and Cu contents with confidence. Our study suggests that the actual chemical composition should be $\text{Li}_{1-z}\text{Cu}_{1-z}^+\text{Cu}_{1+z}^{2+}\text{O}_2$ and Cu^{2+} impurity spins are introduced by Li^+ deficiency along the O-Cu-O dumbbells $\parallel c$ direction. These results should pave the way to a better understanding on this intriguing 1D quantum spin system both theoretically and experimentally.

F.C.C. acknowledges the support from National Science Council of Taiwan under Project No. NSC-95-2112-M-002.

*fcchou@ntu.edu.tw

¹R. Berger, A. Meetsma, S. van Smaalen, and M. Sundberg, *J. Less Common Met.* **175**, 119 (1991).

²S. J. Hibble, J. Kohler, and A. Simon, *J. Solid State Chem.* **88**, 534 (1990).

³T. Masuda, A. Zheludev, A. Bush, M. Markina, and A. Vasiliev, *Phys. Rev. Lett.* **92**, 177201 (2004).

⁴S. Seki, Y. Yamasaki, M. Soda, M. Matsuura, K. Hirota, and Y. Tokura, *Phys. Rev. Lett.* **100**, 127201 (2008).

⁵S. Park, Y. J. Choi, C. L. Zhang, and S.-W. Cheong, *Phys. Rev. Lett.* **98**, 057601 (2007).

⁶A. A. Bush, K. E. Kamentsev, and E. A. Tishchenko, *Inorg.*

Mater. **40**, 44 (2004).

⁷A. S. Moskvin, Y. D. Panov, and S.-L. Drechsler, arXiv:0801.1975 (unpublished).

⁸L. Capogna, M. Mayr, P. Horsch, M. Raichle, R. K. Kremer, M. Sofin, A. Maljuk, M. Jansen, and B. Keimer, *Phys. Rev. B* **71**, 140402(R) (2005).

⁹M. Goiran, M. Costes, J. M. Broto, F. C. Chou, R. Klingeler, E. Arushanov, S.-L. Drechsler, B. Buchner, and V. Kataev, *New J. Phys.* **8**, 74 (2006).

¹⁰O. Prokhnenko, R. Feyerherm, E. Dudzik, S. Landsgesell, N. Aliouane, L. C. Chapon, and D. N. Argyriou, *Phys. Rev. Lett.* **98**, 057206 (2007).